Asymmetric surface plasmon resonances revisited as Fano resonances

Dmitry V. Nesterenko,[1,2,*] Shinji Hayashi,[3,4] and Zouheir Sekkat[3,5,6]

[1]*Diffractive Optics Laboratory, Image Processing Systems Institute RAS – Branch of the FSRC "Crystallography and Photonics" RAS, Samara 443001, Russia*

[2]*Faculty of Information Technology, Samara National Research University, Samara 443086, Russia*

[3]*Optics and Photonics Center, Moroccan Foundation for Science, Innovation and Research, Rabat 10100, Morocco*

[4]*Graduate School of Engineering, Kobe University, Kobe 657-8501, Japan*

[5]*Graduate School of Engineering, Osaka University, Suita 565-0871, Japan*

[6]*Faculty of Sciences, Mohammed V University in Rabat, Rabat 10010, Morocco*

(Received 19 January 2018; revised manuscript received 20 April 2018; published 25 June 2018)

Attenuated total reflection spectra of planar metal-dielectric structures obtained in the Otto and Kretschmann configurations exhibit resonance dips due to excitation of surface-plasmon polaritons. Although the dips have asymmetric line shapes, the asymmetry has not received much attention and the Lorentzian symmetric line shape has commonly been used in the spectral analyses. We analyze the reflectivity spectra of two- and three-layer plasmonic systems based on the electromagnetic and coupled-mode theories, and demonstrate that the asymmetric line shapes can be regarded as the Fano line shapes. In the resonance region, the spectra calculated as Fano line shapes using our approximate expressions are in excellent agreement with those obtained by rigorous electromagnetic calculations. The present formulations of the reflectivity allow us to gain insight into physical origins of characteristic behavior of the plasmonic resonances.

DOI: 10.1103/PhysRevB.97.235437

I. INTRODUCTION

An increasing number of studies in nanophotonics is focused on excitation of different eigenmodes in optical structures. The associated resonance effects such as the field enhancement and narrow resonance features in spectral line shapes are of great interest for both the fundamental and applied sciences. The early studies of the resonance effects in planar multilayer structures were performed on planar plasmonic structures that support surface-plasmon polaritons (SPPs) [1,2]. The plasmonic resonances are characterized by considerably large dissipative losses and low-Q factor that simplifies their experimental observation and analysis. With the increasing demands on high-precision measurements and large field enhancements, the research focus was shifted to high-Q resonances in high refractive index dielectric structures [3]. The research was further extended to metal-dielectric structures that support hybridization of the plasmonic and waveguide modes [4]. This approach allowed engineering of sharp Fano resonances of the required quality factor and line shape [5,6]. Presently, the design and tuning of narrow resonances in plasmonic structures remain demanding tasks that require the development of relevant models for the underlying physical processes.

The studies on the near field enhancement and resonance response at metal-dielectric interfaces are important for a variety of applications, for example creating nanoscale local light sources and generating guided single plasmons in integrated optical circuits [7], enhancement and quenching of fluorescence of single molecules placed in the vicinity of a metal surface [8], and resonant enhancement of the emission rate of optical emitters into the surface plasmons in thin metal films [9] and metal-dielectric-metal slabs [10]. Owing to these resonance properties, simple planar plasmonic structures [11–13], such as insulator-metal-insulator [14] and metal-insulator-metal structures [15], and coupled SPP-waveguide mode structures [6,16–20], are applied to metal-dielectric waveguides [21], sensors [22–25], platforms of surface-enhanced spectroscopies [26–28], and elements for optical computing and imaging [29,30]. In the last decade, the spatial control of SPP modes propagating along metal-dielectric interfaces has been the subject of intensive studies to realize light concentration and scattering suppression [31–34].

It is well known that a metal-dielectric interface can support so-called surface-plasmon polaritons; an SPP is a coupled mode of collective oscillation of free electrons in metal and electromagnetic oscillation that propagates along the interface and decays exponentially away from the interface [1,2]. According to rigorous electromagnetic theory based on solution of Maxwell equations [1,2,35], SPP modes are classified into TM modes and can be excited by p-polarized light. Due to their hybrid nature, SPP modes propagate along the interface with phase velocities lower than that of propagating waves in free space [36]. Therefore, the direct excitation of SPP modes by propagating waves is prohibited and the excitation can be done by waves of reduced phase velocities, such as evanescent waves.

A well-known technique for exciting SPPs in planar structures by light is based on generation of evanescent waves under attenuated total reflection (ATR) conditions [37]. The ATR approaches for exciting SPPs at metal-dielectric interfaces using high-index prisms, which are placed in a close proximity to the metal-dielectric system, were introduced by Turbadar

*dtnesteren@gmail.com

[38,39] in 1959, and by Otto [40] and Kretschmann and Raether [41] in 1968. In the Otto and Kretschmann configurations, which celebrate the 50th anniversary, a *p*-polarized light beam is incident in the prism under angles larger than the critical angle of total reflection; evanescent waves are generated in both the metal and low-index dielectric layers and coupled to a SPP mode at their interface. The coupling efficiency depends on the proximity of the phase velocity of an evanescent wave to that of the SPP mode and takes its maximal value at a certain incidence angle, which is referred to as a resonance angle. Losses induced by the SPP mode lead to the appearance of a resonance dip in the ATR spectra.

The resonance properties of SPP modes and optical properties of the media are efficiently characterized by the ATR spectra in the planar plasmonic structures. Experimental and theoretical angle-scan ATR spectra of the planar plasmonic structures reported in the literature usually exhibit strongly asymmetric resonance line shapes [1,2,35]. However, surprisingly little attention was paid to the asymmetry in the resonance spectra obtained in the Kretschmann and Otto ATR configurations. Using exact electromagnetic theory based on solution of Fresnel equations, Kretschmann [42] obtained a symmetric Lorentzian approximation for the reflection coefficient spectra in a three-layer system in 1971 that was later summarized by Raether [35] in 1988. Despite the discrepancy with theoretical and experimental asymmetrical spectra, this approximation provided a framework for many later studies on SPP modes [26,29,34]. It was only in 2002 that an asymmetric curve-fitting equation for the SPP resonance was derived using a more precise approximation of the three-layer Fresnel equations [43].

Asymmetric resonances are common for many oscillating physical systems [44]. The appearance of asymmetry in the resonance profiles was first explained by Fano in terms of the interference of responses from discrete and continuum states of the systems [45,46]. The interference leads to the resonant enhancement and suppression that correspond to the maximum and minimum in spectral line shapes, respectively. A broad variety of more or less complex plasmonic nanostructures and metamaterials have been reported to exhibit Fano resonances due to mode interaction [47–50]. In plasmonics, Fano resonances in dielectric and metallic nanostructures have also been described using an analogy with a classical system of two coupled mechanical oscillators [5,48,51] and by a formalism of the coupled-mode (CM) theory [52,53]. The CM theory is generally used to describe field and energy flows in resonant systems, such as resonant gratings [54] and plasmonic and photonic structures [29,34,55,56], to provide a deeper insight into the general Fano-like phenomena of mode coupling. Despite recent extensive experimental and theoretical studies on Fano resonances in plasmonic nanostructures and metamaterials, for the angle-scan ATR spectra obtained in the Kretschmann and Otto configurations, no attempt has been made so far to attribute the asymmetry in the line shapes to the Fano resonance. Since the planar ATR configuration is one of the most elemental and fundamental plasmonic structures, understanding of origins of the asymmetric line shapes is of primary importance to further extend its applications.

In this paper, using the exact electromagnetic theory and the CM theory, we study analytically the asymmetric resonances in the spectra of planar two- and three-layer structures that support SPP modes. We show that the reflection coefficients can be decomposed into a nonresonant continuum and a resonant component associated with the SPP excitation, and demonstrate that the Fano line shape arises due to the interference of these components. We derive the same analytical approximations for the Fano resonances from both the exact electromagnetic and CM theories. We analyze field transfer processes in the structures by the CM theory and demonstrate their role in the Fano resonance shifting. The theoretical results are illustrated by rigorous numerical calculations of plasmonic structures based on silver (Ag) and aluminum (Al) at the wavelength of 632.8 nm, which is typical for sensing applications. The revealed fundamental mechanisms of field coupling and field transfer in the Fano-resonant planar plasmonic structures are crucial to analyze and design the structures of higher complexity that support modes of different nature. Our theoretical models based on analytical approaches will be useful for further numerical investigations of resonance structures and can lead to revisiting the traditional approaches for resolving light-matter interactions.

II. FANO RESONANCES AT SINGLE INTERFACES

Since SPPs at single planar dielectric-metal interfaces can be excited by evanescent waves, the fundamental characteristics of SPPs have been investigated using the ATR configurations. The well-known Kretschmann and Otto ATR configurations owe their popularity partly to their structural and implementation simplicity. To reveal the underlying physics associated with the excitation of the SPP modes in these configurations, first we focus on a single dielectric-metal interface, which is the most elemental structure that supports the SPP modes. We study the behavior of the reflection coefficient at the single interface assuming generation of evanescent waves in both the metal and dielectric media, because this process is encountered in these ATR configurations. A key issue of the present analysis is to demonstrate that the reflection coefficient spectra at the single interfaces exhibit the Fano line shape. Although the coefficient itself cannot be measured in this case, its theoretical analysis is indispensable as the first step to demonstrate the Fano resonance in the Kretschmann and Otto configurations.

A. Electromagnetic theory

We start with a brief derivation of a reflection coefficient at a single interface introducing notations used in this paper. Let us consider a general case of a *p*-polarized plane wave incident on an interface I_{12} ($z = 0$) between two semi-infinite homogeneous layers L_1 and L_2 with permittivities ε_1 and ε_2, respectively, as shown in Fig. 1. Let us suppose that the structure is uniform in the x and y directions. In the coordinate system shown in Fig. 1, the harmonic magnetic fields in the structure can be written as $\mathbf{H}^{(j)} = (0, H_y^{(j)}, 0)\exp(-i\omega t)$, where the index j denotes the layer number, e.g., $j = 1$ for the dielectric and $j = 2$ for the metal, and ω is an angular frequency. Electromagnetic waves are assumed to propagate in the x-z plane, therefore the total field $\psi = H_y^{(j)}(x,z)$ is uniform in the y direction. The steady-state wave equation

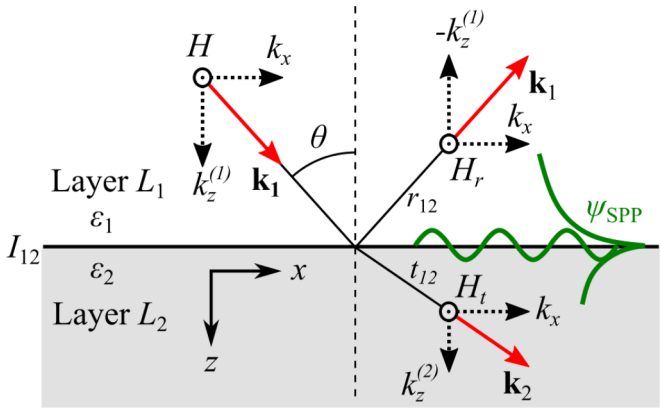

FIG. 1. Reflection and refraction of light at an interface between two semi-infinite layers.

for the complex amplitude ψ of the total field is represented by a scalar Helmholtz equation

$$\frac{\partial^2\psi}{\partial x^2}+\frac{\partial^2\psi}{\partial z^2}+k_0^2\varepsilon(z)\psi=0, \tag{1}$$

where $k_0=\omega/c=2\pi/\lambda_0$ is the free-space wave number, c is the speed of light in vacuum, and λ_0 is the wavelength in the free space. The equation for the incident plane wave propagating in L_1 can be written as $H_y(x,z)=u\exp[ik_0(\alpha x+\beta_1 z)]$, where u is the complex amplitude of the incident wave, and the z component of the propagation constant β_1 is given by $\beta_1=\sqrt{\varepsilon_1-\alpha^2}$. For a propagating wave incident at an angle θ to the surface normal, $\beta_1=\sqrt{\varepsilon_1}\cos\theta$ and the x component of the propagation constant is given by $\alpha=\sqrt{\varepsilon_1}\sin\theta$. For a plane wave propagating along the x direction with $\alpha^2>\varepsilon_1$, β_1 has a nonzero imaginary part that results in the exponential decay of the wave amplitude in the z direction. Such plane waves are referred to as evanescent waves.

When a plane wave is incident on the interface I_{12}, two outgoing plane waves are generated. One is reflected back to L_1, and the second is transmitted to L_2. The total field $\psi_\alpha(x,z)$ for a particular α being a solution of Eq. (1) is represented by a sum of the incident and reflected waves in L_1 and by the transmitted wave in L_2 as

$$\psi_\alpha(x,z)=\begin{cases}H(x,z)+H_r(x,z), z\leqslant 0,\\ H_t(x,z), z\geqslant 0.\end{cases} \tag{2}$$

Therefore, the fields of the reflected H_r and transmitted H_t waves are written as $H_r(x,z)=r_{12}(\alpha)u\exp[ik_0(\alpha x-\beta_1 z)]$ and $H_t(x,z)=t_{12}(\alpha)u\exp[ik_0(\alpha x+\beta_2 z)]$ with the complex coefficients r_{12} and t_{12}, respectively. These complex coefficients can be interpreted as responses of the optical system to the external excitation. In experiments, reflectance or transmittance spectra are obtained by measuring the intensities of the reflected and transmitted light as a function of the incidence angle or the in-plane propagation constant.

Let us define an operator $\hat{M}$ corresponding to Eq. (1) by

$$\hat{M}\psi=\left[\frac{\partial^2}{\partial z^2}+k_0^2\varepsilon(z)\right]\psi.$$

In general, if $\hat{M}$ has a discrete spectrum, a discrete eigenmode of $\hat{M}$ numbered by integer index l is defined as $\psi_l(x,z)=\psi_l(z)\exp(i\gamma_l k_0 x)$ that satisfies the eigenvalue equation

$$\hat{M}\psi_l(x,z)=(\gamma_l k_0)^2\psi_l(x,z), \tag{3}$$

where $\psi_l(z)$ and $(\gamma_l k_0)^2$ are the discrete eigenvector and eigenvalue, respectively. It can be easily demonstrated that the response of a discrete mode with propagation constant γ_l excited by the incident plane wave H with the propagation constant α has an asymptotic resonance behavior expressed as $(\gamma_l^2-\alpha^2)^{-1}H$ [48].

In the case of metal-dielectric system $\mathrm{Re}\{\varepsilon_1\}\mathrm{Re}\{\varepsilon_2\}<0$ and $\mathrm{Re}\{\varepsilon_1+\varepsilon_2\}<0$, SPP modes $\psi_{SPP}(x,z)$ are discrete eigenmodes of $\hat{M}$ with the eigenvalue $(\gamma_{SPP}k_0)^2$, where magnetic fields associated with the mode can be written as $\psi_{SPP}^{(j)}=\exp(ik_{SPP}x)\exp(-b_j|z|)$. The SPP dispersion relation between the wave vector $k_{SPP}=\gamma_{SPP}k_0$ and ω is given by $k_{SPP}=(\omega/c)[\varepsilon_1\varepsilon_2/(\varepsilon_1+\varepsilon_2)]^{1/2}$. Moreover, b_j given as $b_j=(\omega/c)[-\varepsilon_j^2/(\varepsilon_1+\varepsilon_2)]^{1/2}$ takes positive values in metal-dielectric systems. The SPP field amplitude has its maximum at the interface I_{12}, exponentially decays with the distance from the interface in both media, and disappears at $|z|\to\infty$, as schematically shown in Fig. 1. Taking the mode attenuation into account, the complex propagation constant is represented as $\gamma_{SPP}=\gamma'_{SPP}+i\gamma''_{SPP}$. The real part γ'_{SPP} characterizes the mode phase velocity, and γ''_{SPP} is the extinction coefficient. To study the response of the two-layer system associated with the excitation of an SPP mode, we concentrate on generation of evanescent waves in both media under the conditions $\alpha^2>\mathrm{Re}\varepsilon_1,\mathrm{Re}\varepsilon_2$.

To discover the resonance behavior of the response of the considered two-layer system, the propagation of evanescent waves is studied in the vicinity of SPP propagation constant γ'_{SPP}. The generalized Fresnel coefficients can be found using the 2×2 transfer-matrix method [57] based on the steady-state solution of a system of linear equations for the complex amplitudes of plane waves propagating in a stratified medium. The equations represent continuity conditions for the magnetic field $\psi_\alpha(x,z)$ and its derivatives along interfaces between layers. The forward and backward reflection coefficients, r_{ij} and r_{ji}, and transmission coefficient t_{ij} are given for some adjacent layers L_i and L_j as

$$r_{ij}=\frac{\beta_i/\varepsilon_i-\beta_j/\varepsilon_j}{\beta_i/\varepsilon_i+\beta_j/\varepsilon_j},\quad r_{ji}=-r_{ij},\quad \text{and } t_{ij}=1+r_{ij}. \tag{4}$$

For $\alpha^2>\mathrm{Re}\,\varepsilon_i,\mathrm{Re}\,\varepsilon_j$, both β_i and β_j have nonzero imaginary parts and the incident, reflected, and transmitted plane waves are evanescent in the z direction in both layers. For this reason this spectral region is hereafter referred to as an evanescent region. In contrast to the case of a propagating wave, in which the magnitude of the wave is constant with distance, the complex amplitudes of the generated evanescent waves are defined by the reflection and transmission coefficients at the interface. Thus, $|r_{ij}|^2$ and $|t_{ij}|^2$ may be regarded as the coefficients of near field enhancement along the x axis for the generated evanescent fields at the frontal (in respect to the incoupling wave) and outer interfaces, respectively. In the evanescent region, the energy is not transferred in the z direction, whereas the evanescent waves are capable of

generating a field in a dense medium placed in the vicinity. This phenomenon of a field transfer process is described in optics as an evanescent-field coupling, where the coupling degree is characterized by the reflection and transmission coefficients.

In the experiments, the spectra of reflectivity $|r_{ij}|^2$ and transmission $|t_{ij}|^2$ of the propagation waves can be registered by a detector. In the evanescent region, the direct estimation of the near field enhancement of the evanescent waves is not possible. To characterize the near field enhancement, the generated evanescent fields can be converted to propagating waves in other media by the use of coupling devices. This approach transforms the spectra of the near field enhancement based on the in-plane propagation constant into the angular spectra of the intensity of propagating waves.

In the evanescent region, r_{ij} can be written using Eq. (4) in the form

$$r_{ij} = \frac{\gamma_{\mathrm{SPP}}^2(\varepsilon_i+\varepsilon_j)^2 - \left(\varepsilon_i^2+\varepsilon_j^2\right)\alpha^2 + 2\varepsilon_i\varepsilon_j\alpha^2\sqrt{1+(\varepsilon_i+\varepsilon_j)\left(\gamma_{\mathrm{SPP}}^2-\alpha^2\right)/\alpha^4}}{(\varepsilon_j-\varepsilon_i)(\varepsilon_i+\varepsilon_j)\left(\gamma_{\mathrm{SPP}}^2-\alpha^2\right)}. \tag{5}$$

Under the assumption that the difference between α and γ_{SPP} is small and $(\gamma_{\mathrm{SPP}}^2-\alpha^2)/\alpha^4 \to 0$, r_{ij} can be approximated in the vicinity of resonance $\alpha \to \gamma'_{\mathrm{SPP}}$ as well as in the limit $\alpha \to \infty$ using lower-order terms of a Taylor series for the square root in Eq. (5). This approximation results in the decomposition of r_{ij} as

$$\tilde{r}_{ij} = r_{ij}^c + r_{ij}^{\mathrm{SPP}} = r_{ij}^c\,\chi, \tag{6}$$

where

$$r_{ij}^c = \frac{\varepsilon_j-\varepsilon_i}{\varepsilon_i+\varepsilon_j} + \frac{\varepsilon_i+\varepsilon_j}{\varepsilon_j-\varepsilon_i}\frac{\gamma_{\mathrm{SPP}}^2}{\alpha^2} \tag{7}$$

corresponds to a broad continuum component originating from the nonresonant reflection by the interface, in which the amplitude and phase are slowly changing near $\alpha = \gamma'_{\mathrm{SPP}}$, and the component $r_{ij}^{\mathrm{SPP}} = 2\gamma_{\mathrm{SPP}}p_{ij}/(\gamma_{\mathrm{SPP}}^2-\alpha^2)$ is characterized by fast changes of the amplitude and phase and corresponds to the resonant outcoupling from the discrete SPP modes. A single evanescent wave excites two SPP modes of propagation constants γ_{SPP} and $-\gamma_{\mathrm{SPP}}$ that propagate in x and $-x$ directions, respectively. As a result, the component r_{ij}^{SPP} is composed of the responses from these two SPP modes as $r_{ij}^{\mathrm{SPP}} = p_{ij}/(\alpha+\gamma_{\mathrm{SPP}}) - p_{ij}/(\alpha-\gamma_{\mathrm{SPP}})$, where

$$p_{ij} = 2\gamma_{\mathrm{SPP}}^3(\varepsilon_j-\varepsilon_i)^{-1} \tag{8}$$

is the complex amplitude of a single SPP mode response.

Using Eq. (6), the ratio χ of the total optical response of a two-layer system to the continuum response is found as

$$\chi = \tilde{r}_{ij}/r_{ij}^c = 1 + \frac{d_{ij}}{\gamma_{\mathrm{SPP}}^2-\alpha^2} \tag{9}$$

with

$$d_{ij} = 2\gamma_{\mathrm{SPP}}p_{ij}/r_{ij}^c = \frac{4w\alpha^2\gamma_{\mathrm{SPP}}^4}{(\varepsilon_j+\varepsilon_i)\left(\alpha^2+w\gamma_{\mathrm{SPP}}^2\right)},$$

$$\text{and}\quad w = \left(\frac{\varepsilon_j+\varepsilon_i}{\varepsilon_j-\varepsilon_i}\right)^2, \tag{10}$$

where d_{ij} is the ratio of response from the discrete SPP modes to the continuum component. Assuming $\gamma''_{\mathrm{SPP}} \ll \gamma'_{\mathrm{SPP}}$ and neglecting the second-order contribution, Eq. (9) can be rewritten as

$$\chi = 1 + \frac{q}{k+i} \tag{11}$$

where $k = [(\gamma'_{\mathrm{SPP}}+\Delta)^2-\alpha^2]/\Gamma$ is the reduced frequency, $\Delta = -\gamma''^2_{\mathrm{SPP}}/(2\gamma'_{\mathrm{SPP}})$ is the shift in the resonance position caused by the damping of the discrete mode, $\Gamma = 2\gamma'_{\mathrm{SPP}}\gamma''_{\mathrm{SPP}}$ is the resonance width, and $q = d_{ij}/\Gamma$ is given by the ratio of the normalized amplitude of the discrete mode to the width Γ. In the general case of complex $q = q' + iq''$, the squared module of the ratio of total and continuum responses is given by the resonance factor

$$\sigma = |\chi|^2 = \frac{(k+q')^2+(1+q'')^2}{1+k^2}, \tag{12}$$

which comprises a sum of Fano and Lorentzian functions that depend on losses in the materials [46,48]. The parameter d_{ij} is supposed to change slowly with α, so q' and q'' can be considered as constants in the region of resonance. The Lorentzian term influences the interference contrast. This influence can be minimized by finding optimal material parameters. For instance, when $q'' = -1$ and q' is nonzero, the overall response of the system is determined only by the discrete mode at the resonance. In this case, the Lorentzian term disappears, and σ is described by the Fano function with maximal contrast of the line shape. For the lossless case ($\gamma''_{\mathrm{SPP}} = 0$), the resonance width is zero ($\Gamma = 0$), and $\sigma = \infty$ at the resonance. If there is no interaction with the discrete mode or it has no response, i.e., $q = 0$, no resonance interference can be observed, and the response becomes $\sigma = 1$.

Basically, σ represents the near field enhancement normalized to that of the nonresonant continuum. The appearance of the resonant and nonresonant components in the total response, which is revealed by the approximation (6), is intrinsic to metal-dielectric interfaces. Their direct separation from the observed resonance spectra in two-layer structures may not be possible. Therefore, σ is an analytical function that demonstrates the formation of Fano line shape in the total response spectra.

The near field enhancement of the dielectric-metal interface around the SPP resonance is determined by the interference of a sharp resonance response of the discrete SPP mode and a broad nonresonant continuum, resulting in a Fano-type resonance spectral line shape:

$$|\tilde{r}_{ij}|^2 = \left|r_{ij}^c\right|^2\frac{(k+q')^2+(1+q'')^2}{1+k^2}. \tag{13}$$

This expression is similar to the general formula for the electromagnetic response of a system with losses [48].

In the vicinity of resonance $\alpha \to \gamma'_{\mathrm{SPP}}$, assuming $\gamma'_{\mathrm{SPP}} \gg 0$ we can neglect the response from the SPP mode of the propagation constant $-\gamma'_{\mathrm{SPP}}$ that propagates in the opposite direction. The following simple approximation for χ is obtained using the decomposition of Eq. (9) taking into account the response from the SPP mode propagating in the forward direction only [50]:

$$\tilde{\chi} = \frac{\alpha - \gamma_{\mathrm{zero}}}{\alpha - \gamma_{\mathrm{pole}}}, \tag{14}$$

where

$$\gamma_{\mathrm{pole}} = \gamma_{\mathrm{SPP}} \text{ and } \gamma_{\mathrm{zero}} = \gamma_{\mathrm{SPP}} + p_{ij}/r^c_{ij} \tag{15}$$

are the pole and zero parameters of the function $\tilde{\chi}$, respectively. Therefore, the approximation (6) is written as

$$\tilde{r}_{ij} = r^c_{ij} \frac{\alpha - \gamma_{\mathrm{SPP}}\left[1 + p_{ij}/\left(r^c_{ij}\gamma_{\mathrm{SPP}}\right)\right]}{\alpha - \gamma_{\mathrm{SPP}}}. \tag{16}$$

Using the approximation (16) and assuming complex $\gamma_{\mathrm{pole}} = \gamma'_{\mathrm{pole}} + i\gamma''_{\mathrm{pole}}$ and $\gamma_{\mathrm{zero}} = \gamma'_{\mathrm{zero}} + i\gamma''_{\mathrm{zero}}$, the near field enhancement for the dielectric-metal interfaces is represented in the form of asymmetric Fano formula

$$|\tilde{r}_{ij}|^2 = |r^c_{ij}|^2 \frac{(\alpha - \gamma'_{\mathrm{zero}})^2 + \gamma''^2_{\mathrm{zero}}}{(\alpha - \gamma'_{\mathrm{pole}})^2 + \gamma''^2_{\mathrm{pole}}}. \tag{17}$$

According to Eq. (15), γ'_{zero} is displaced from γ'_{pole} that leads to an asymmetric Fano line shape of $|\tilde{r}_{ij}|^2$. Since $d_{ij} = d_{ji}$, the displacement occurs in the same direction for both the dielectric-metal interfaces ($\varepsilon_i > 0$, $\varepsilon_j < 0$) and metal-dielectric interfaces ($\varepsilon_i < 0$, $\varepsilon_j > 0$). Moreover, for most of the combinations of dielectrics and metals d_{ij} takes a negative value in the visible region and consequently γ'_{zero} is displaced to a value lower than γ'_{pole}.

It should be stressed here that the approximations (13) and (17) imply that the asymmetric Fano resonance line shape is inherent in the near field enhancement spectra of two-layer metal-dielectric structures. The Fano resonance appears due to the interference between a resonant response of the SPP mode and nonresonant reflection from the metal-dielectric interface. In what follows, we clarify the underlying physics of the resonance by establishing an analogy between the electromagnetic and CM theories.

B. Coupled-mode theory

Optical spectra observed in plasmonic structures can be obtained by exact electromagnetic theory. The structures considered in the present paper can be described analytically. For a variety of more complex structures, numerical methods should be implemented. In general, numerical methods applied to electromagnetic field calculations are usually time and resource consuming. Moreover, the field solutions do not provide a deep understanding on the dynamics of underlying processes. Therefore, the CM theory was developed to provide a general description of energy flows to and from resonators [52].

The CM approach in optics was implemented for analysis of Fano resonances in terms of interaction of electromagnetic fields in the form of discrete normal modes; incident, reflected, and transmitted plane waves; and diffraction orders of diffraction gratings [53,54,58]. In the CM models, the plasmonic resonances are represented as results of energy transfer in optical processes such as direct field scattering and incoupling to and outcoupling from SPP modes. These energy flows are described by parameters of the model. The CM theory provides numerical methods much faster than conventional ones and allows us to calculate fields that fit to those obtained by the exact theory. However, in the numerous previous implementations of the CM theory to resonant planar one- and two-dimensional structures [29,34,53–55,58], the transfer coefficients for the CM models are obtained by fitting the CM approximations to the numerical calculations by exact electromagnetic theory. Still, no good analytical representation for the coupling coefficients has been presented yet.

In this subsection, we develop a one-dimensional spatial formulation of the CM theory and derive basic equations for the complex amplitude of a SPP mode propagating along the interface in a two-layer system. As a starting point, consider a field solution of the mode ψ_{SPP} as $\psi_{\mathrm{SPP}} = c(\alpha,x)\exp(ik_0\gamma_{\mathrm{SPP}}x)$, where an envelope function $c(\alpha,x)$ is a slowly varying function defined after removing the fast $\exp(ik_0\gamma_{\mathrm{SPP}}x)$ dependence of the field. Neglecting the first-order derivative of $c(\alpha,x)$, the dynamic equation for ψ_{SPP} can be approximated as

$$\frac{1}{ik_0\gamma_{\mathrm{SPP}}}\frac{\partial\psi_{\mathrm{SPP}}}{\partial x} = \psi_{\mathrm{SPP}}. \tag{18}$$

In contrast to the conventional formulation of the CM theory [52], the coefficient $ik_0\gamma_{\mathrm{SPP}}$ is placed on the left-hand side of Eq. (18) to correctly define coupling with external fields. The mode ψ_{SPP} can be excited by incoupling of an evanescent wave H:

$$\frac{1}{ik_0\gamma_{\mathrm{SPP}}}\frac{d\psi_{\mathrm{SPP}}}{dx} = \psi_{\mathrm{SPP}} + \kappa H, \tag{19}$$

where κ is a coefficient expressing the coupling strength between the mode and the incoupling (outcoupling) wave. The resonant excitation of the SPP mode by the incoupling wave is fully described by Eq. (19).

The outcoupled evanescent wave H_r is composed of a nonresonant component generated by the incoupling wave H with the coupling coefficient r^c_{ij} and a resonant component as a result of outcoupling of the mode ψ_{SPP} with coupling coefficient $-\kappa$. The expression for H_r may be written as follows:

$$H_r = r^c_{ij}H - \kappa\psi_{\mathrm{SPP}}. \tag{20}$$

Assuming that the incoupling wave has a propagation constant α along the x axis, $H \propto \exp(ik_0\alpha x)$, then the mode ψ_{SPP} has the same propagation constant, and we find, from Eq. (19), that the mode spectrum is represented by a Lorentzian

$$\psi_{\mathrm{SPP}} = \frac{\gamma_{\mathrm{SPP}}}{\alpha - \gamma_{\mathrm{SPP}}}\kappa H. \tag{21}$$

According to Eq. (21), the pole of ψ_{SPP} is fixed at γ_{SPP}, because the incoupling of an evanescent wave does not perturb the mode. Therefore, the mode losses are not affected by

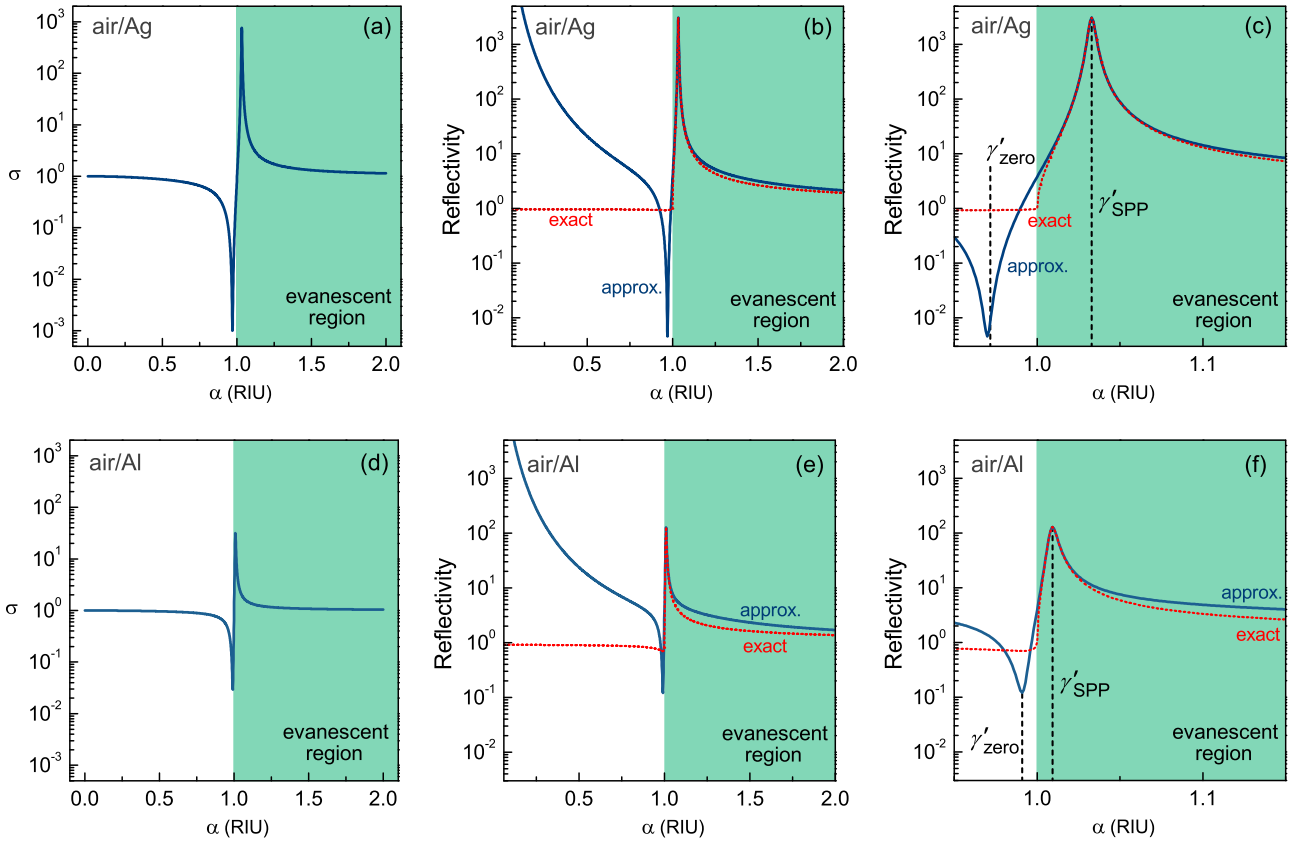

FIG. 2. The resonant behavior of the resonance factor σ for (a) air/Ag and (d) air/Al interfaces. (b, e) Comparison of the exact solution $|r_{ij}(\alpha)|^2$ (dotted lines) with the approximation $|\tilde{r}_{ij}(\alpha)|^2$ (solid lines) for (a–c) air/Ag and (d–f) air/Al interfaces. (c, f) The expanded scale near the resonance region. The filled area corresponds to the evanescent region.

coupling processes and include only the SPP intrinsic losses γ''_{SPP}. The overall coupling coefficient $\tilde{r}_{ij} \equiv H_r/H$ of the system can be evaluated for an arbitrary incoupling wave by substituting Eq. (21) into Eq. (20):

$$\tilde{r}_{ij} = r^{\mathrm{c}}_{ij}\frac{\alpha - \gamma_{\mathrm{SPP}}\left(1 + \kappa^2/r^c_{ij}\right)}{\alpha - \gamma_{\mathrm{SPP}}}. \tag{22}$$

According to Eq. (22), $\tilde{r}_{ij}$ depends on the mode propagation constant, nonresonant coupling coefficient, and coupling coefficient κ. The solution (22) can be represented in a form consistent with Eq. (16). Here, the zero and pole parameters of a two-layer system are $\gamma^{\mathrm{CM}}_{\mathrm{zero}} = \gamma_{\mathrm{SPP}}(1 + \kappa^2/r^c_{ij})$ and $\gamma^{\mathrm{CM}}_{\mathrm{pole}} = \gamma_{\mathrm{SPP}}$, respectively. Hence, comparing $\gamma^{\mathrm{CM}}_{\mathrm{zero}}$ and $\gamma^{\mathrm{CM}}_{\mathrm{pole}}$ with those in Eq. (15), we find an expression for κ as

$$\kappa = \sqrt{p_{ij}/\gamma_{\mathrm{SPP}}} = \gamma_{\mathrm{SPP}}\sqrt{\frac{2}{\varepsilon_j - \varepsilon_i}}. \tag{23}$$

Thus, κ is proportional to the SPP propagation constant. Neglecting small imaginary parts of the permittivities and propagation constant, κ takes imaginary values for dielectric-metal interfaces ($\varepsilon_i > 0$, $\varepsilon_j < 0$) and real values for metal-dielectric interfaces ($\varepsilon_i < 0$, $\varepsilon_j > 0$). The phase of κ determines a phase shift brought by the coupling process.

The above reformulation of the conventional CM description of incoupling dynamics of a SPP mode in the form (19) provides a general expression for the two-layer system response given by Eq. (22). This general expression coincides with Eq. (16) obtained analytically using the exact electromagnetic theory.

C. Comparison of numerical results

To verify the validity of the approximation given by Eq. (13), numerical results for the air/Ag and air/Al interfaces at $\lambda_0 = 632.8$ nm are presented in Fig. 2. Permittivities of air, Ag, and Al were taken as 1.0, $-15.886 + 1.074i$, and $-51.410 + 18.446i$, respectively [59,60]. Figures 2(a) and 2(d) show the dependence of the resonance factor σ on α, when α is changed from zero to two refractive index units (RIU). As can be seen from the figures, σ exhibits a sharp Fano-like line shape for both the air/Ag and air/Al interfaces. In Figs. 2(b), 2(c), 2(e), and 2(f), results obtained by the exact solution $|r_{ij}(\alpha)|^2$ [Eq. (5)] are compared with those obtained from the approximate expression $|\tilde{r}_{ij}(\alpha)|^2$ [Eq. (13)]. In the evanescent region ($\alpha > 1$ RIU), we observe overall good fits of the approximation to the exact solution. Note that $|\tilde{r}_{ij}(\alpha)|^2$ exhibits a Fano line shape modulated by the slowly varying $|r^c_{ij}(\alpha)|^2$ coefficient. The positions of the peak and minimum in the approximation curves coincide with those of σ spectra. In the evanescent region, the maximum values of near field enhancement of 3108.1 and 126.7 are achieved for air/Ag and air/Al cases, respectively, due to the resonant excitation of SPP modes, whereas the values of continuous response $|r^c_{ij}(\alpha)|^2$ are 4.1 and 3.8, respectively.

TABLE I. Fano resonance parameters for the air/Ag and air/Al interfaces.

	$\gamma_{pole} = \gamma_{SPP}$ (RIU)	γ_{zero} (RIU)	α_{peak} (RIU)	Peak value	α_{dip} (RIU)	Minimum value	Γ (RIU)
Air/Ag	$1.03288 + 0.00233i$	$0.9720 - 0.0018i$	1.0330	765.1	0.9700	0.001	0.00481
Air/Al	$1.00871 + 0.00317i$	$0.9914 - 0.0030i$	1.0093	31.9	0.9910	0.029	0.00630

The propagation constants for the SPP modes, resonance width Γ, pole γ_{pole}, and zero γ_{zero} parameters are summarized in Table I. The lower imaginary part of γ_{pole} in the air/Ag case results in a narrower width. The peak position α_{peak} and minimum position α_{dip} of exact solutions are approximated very well by γ'_{pole} and γ'_{zero}, respectively. The amplitude of the Fano line shape defined by the difference between the maximum and minimum values is smaller by two orders of magnitude for the air/Al case as compared to the air/Ag case due to higher attenuation of the mode. In the radiative region ($\alpha < 1$ RIU), the exact solution exhibits entirely different and strongly nonresonant behavior. In this region, Eq. (5) is not valid, as the square root in Eq. (5) is expressed to correctly treat the negative values in the evanescent region.

From the results presented above, it is clear that in the evanescent region the near field enhancement spectra obtained from the exact calculations are very well approximated by the Fano resonance line shapes. The minimum values in σ spectra for the considered metals are located outside the evanescent region, and only the resonance peaks are observed in the spectra of exact solutions.

The difference in the approximated and exact data that we observe in Fig. 2 is originated from the sum of higher-order terms of a Taylor series for the square root in Eq. (5) that was discarded in the approximation (6). According to Eq. (5), this sum is proportional to both permittivities of materials in the two-layer structure. As the permittivity of Al is around three times as high as that of Ag, the approximation in the Ag case is much better.

III. FANO RESONANCES IN THE KRETSCHMANN AND OTTO CONFIGURATIONS

In the previous section, we demonstrated that the resonance response of a single dielectric-metal interface exhibits the asymmetric line shape as a result of Fano interference between the nonresonant and resonant components of the reflection coefficient. The appearance of the resonant component is straightforward: it is based on resonant excitation of the SPP mode. Analysis of field transfer processes by the CM theory showed that the nonresonant component arises independently from the resonant one to fulfill off-resonance boundary conditions. Based on the approaches developed for the single interface, we will discover the physical interpretation and underlying transfer processes for the SPP excitation in the conventional planar three-layer structures in the Otto and Kretschmann configurations to verify the conformity of their asymmetric ATR resonances to the Fano line shapes.

A. Electromagnetic theory

Under the ATR conditions, SPPs are excited by evanescent waves generated by a high-index prism placed in the vicinity of a metal-dielectric two-layer structure. There are two possible ways of interconnecting the prism with the two-layer structure. If the prism is placed at the side of the dielectric layer, the hybrid structure is referred to as the Otto configuration. If the prism is attached to the metal layer side, the hybrid structure is referred to as the Kretschmann configuration. Both configurations can be represented schematically by three-layer structures, in which the prism and environment are denoted as semi-infinite layers L_0 and L_2, respectively; the spacer layer of a finite thickness h separates the layers L_0 and L_2 and is denoted as L_1 as depicted in Fig. 3. Therefore, the spacer layer L_1 is a dielectric in the Otto configuration and a metal in the Kretschmann configuration.

In general, the overall reflection coefficient r_{012} of a three-layer system for $\alpha = \sqrt{\varepsilon_0}\sin\theta$ is given by [35]

$$r_{012} = \frac{r_{01} + r_{12}\, v^2}{1 + r_{01}\, r_{12}\, v^2}, \tag{24}$$

where r_{01} corresponds to the complex coefficient of the direct plane-wave reflection at the prism-spacer layer interface, and $v = \exp(ik_0\beta_1 h)$ can be regarded as a coefficient that characterizes the decay of evanescent waves excited under ATR conditions in the layer L_1 with distance between the I_{01} and I_{12} interfaces. The decay is expected to be stronger when the layer L_1 is thicker.

In both configurations, an optical response of the SPP mode ψ_{SPP} excited in three-layer structures by p-polarized light is observed as a surface-plasmon resonance (SPR) dip in reflectivity spectra. The dip appears as a result of light energy redistribution to ψ_{SPP} propagating along the metal-dielectric interface I_{12} by means of the evanescent waves coupling. As we showed in the previous section, the resonance response r_{12} of SPP mode excitation at the metal-dielectric interface can

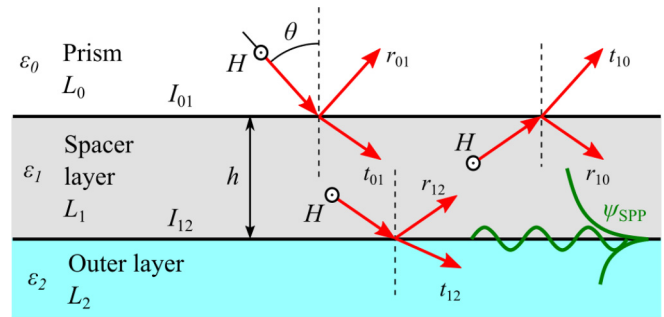

FIG. 3. Reflection and refraction processes at interfaces in three-layer systems.

be represented in the form of Eq. (6) using the Fano formula given by Eq. (11) as $\tilde{r}_{12} = r^c_{12}[1 + q(k+i)^{-1}]$. By substituting $r_{12} \approx \tilde{r}_{12}$ into Eq. (24) the total reflection coefficient r_{012} is thus approximated as

$$\tilde{r}_{012} = r^c_{012}\chi_3, \tag{25}$$

where a resonance factor χ_3 is written for the three-layer system as

$$\chi_3 = \frac{k + i + a/\Gamma}{k + i + b/\Gamma} \tag{26}$$

with

$$\begin{aligned} a &= 2\gamma_{\mathrm{SPP}} v^2 p_{12}\left(r_{01} + r^c_{12}v^2\right)^{-1}, \\ b &= 2\gamma_{\mathrm{SPP}} r_{01} v^2 p_{12}\left(1 + r_{01}r^c_{12}v^2\right)^{-1}, \\ r^c_{012} &= \left(r_{01} + r^c_{12}v^2\right)/\left(1 + r_{01}r^c_{12}v^2\right). \end{aligned} \tag{27}$$

Here, r^c_{012} is a complex amplitude of the continuum response from the three-layer structure as a result of nonresonant field transfer in the structure.

The approximation of reflectivity for the three-layer stack $|\tilde{r}_{012}|^2$ is obtained using Eq. (25) as a sum of asymmetric Fano and symmetric Lorentzian functions:

$$|\tilde{r}_{012}|^2 = \left|r^c_{012}\right|^2 \frac{(k_3 + q'_3)^2 + (1 + q''_3)^2}{k_3^2 + 1}, \tag{28}$$

where $k_3 = [(\gamma'_{\mathrm{SPP}} + \Delta)^2 - \alpha^2 + b']/(\Gamma + b'')$ is the reduced frequency for the three-layer stack, $q_3 = (a - b)/(\Gamma + b'')$, $b = b' + ib''$, and $q_3 = q'_3 + iq''_3$. From Eq. (28) we see that compared to a two-layer metal-dielectric system the resonance position $[(\gamma'_{\mathrm{SPP}} + \Delta)^2 + b']^{1/2}$ and width $\Gamma + b''$ of the three-layer structure are modified by b' and b'', respectively. As follows from Eq. (27), b is proportional to v^2 when $|v^2| \ll 1$. Theoretically, we can predict that the width can be brought to zero, when the parameters of the structure are selected to realize $b'' = -\Gamma$. The Fano component arises from the interference between a response of the discrete SPP mode and a continuum response from the three-layer structure. To increase the resonance contrast, the Lorentzian component can be tuned to zero by optimizing h that affects v^2 to achieve $q''_3 = -1$.

Under an assumption of $\gamma'_{\mathrm{pole}} \gg 0$, the approximation $\tilde{\chi}_3$ of χ_3,

$$\tilde{\chi}_3 = \frac{\alpha - \gamma_{3,\mathrm{zero}}}{\alpha - \gamma_{3,\mathrm{pole}}}, \tag{29}$$

obtained from Eq. (26) gives the pole $\gamma_{3,\mathrm{pole}}$ and zero $\gamma_{3,\mathrm{zero}}$ resonance parameters:

$$\begin{aligned} \gamma_{3,\mathrm{pole}} &= \left(\gamma^2_{\mathrm{SPP}} + b\right)^{1/2}, \\ \gamma_{3,\mathrm{zero}} &= \gamma_{3,\mathrm{pole}} + (a - b)\gamma^{-1}_{3,\mathrm{pole}}/2. \end{aligned} \tag{30}$$

In the case of small decay coefficient v or small nonresonant component r^c_{12}, the approximations of $\gamma_{3,\mathrm{pole}}$ and $\gamma_{3,\mathrm{zero}}$ can be found as

$$\begin{aligned} \tilde{\gamma}_{3,\mathrm{pole}} &= \gamma_{\mathrm{SPP}} + r_{01}v^2 p_{12}, \\ \tilde{\gamma}_{3,\mathrm{zero}} &= \gamma_{\mathrm{SPP}} + v^2 p_{12}/r_{01}. \end{aligned} \tag{31}$$

Additionally, the continuum component r^c_{012} in Eq. (27) is mainly determined by the reflection coefficient at the first interface and can be approximated by $\tilde{r}^c_{012} \approx r_{01}$. In this case, the total reflectivity is given by $\tilde{r}_{012} = r_{01}\tilde{\chi}_3$. For the Otto configuration, $|r_{01}|^2 = 1.0$ in the ATR region that simplifies Eq. (28) to $\tilde{r}_{012} = \tilde{\chi}_3$. According to Eq. (31), an increase of the decay v^2 leads to increases of shifts of zero $\tilde{\gamma}_{3,\mathrm{zero}}$ and pole $\tilde{\gamma}_{3,\mathrm{pole}}$ resonance positions. The final approximation of the total reflection coefficient $\tilde{r}_{012}$ spectra around $\alpha = \gamma'_{\mathrm{SPP}}$ can be expressed using Eq. (29) as

$$\tilde{r}_{012} = r_{01}\frac{\alpha - \gamma_{\mathrm{SPP}}\left(1 + \frac{v^2 p_{12}}{r_{01}\gamma_{\mathrm{SPP}}}\right)}{\alpha - \gamma_{\mathrm{SPP}}\left(1 + \frac{r_{01}v^2 p_{12}}{\gamma_{\mathrm{SPP}}}\right)}. \tag{32}$$

This approximation of SPR spectra exhibits an asymmetric Fano line shape, when its zero and pole resonance parameters defined by Eq. (31) have different real parts. The differences between the resonance parameters, as well as between their shifts from γ_{SPP}, are governed by $r_{01} \neq 1$ and losses of the SPP mode. Kretschmann [42] and Raether [35] obtained a symmetric Lorentzian approximation by assumptions $\mathrm{Re}\, r_{01} = \mathrm{Re}\, r^{-1}_{01}$ and $\mathrm{Im}\, r_{01} = -\mathrm{Im}\, r^{-1}_{01}$, which are correct only in the Otto configuration when $|r_{01}|^2 = 1$. In this case, the nonzero imaginary part of r_{01} induces different changes to the real parts of the zero and pole resonance parameters only for nonzero γ''_{SPP}. In their treatments, the neglect of the SPP mode losses resulted in the equal real parts of the zero and pole resonance parameters and in the Lorentzian line shape of SPR dip. In the Kretschmann configuration, incident light energy dissipates at the prism-metal interface due to losses and gives $|r_{01}|^2 < 1$. According to Eq. (31), this fact unconditionally implies the difference in the real parts of the pole and zero parameters. Therefore, the losses in the system play the main role in generating an asymmetric Fano line shape.

Under ATR conditions, the decay coefficient v decreases with increasing spacer layer thickness h, and $v^2 \to 0$ for large h. According to Eq. (31), the zero $\tilde{\gamma}_{3,\mathrm{zero}}$ and pole $\tilde{\gamma}_{3,\mathrm{pole}}$ resonance parameters approach the γ_{SPP} value that results in $\tilde{\chi}_3 \to 1$. In this case, $\tilde{r}_{012} \to r_{01}$, and the resonance dip disappears. When h decreases, the difference between $\tilde{\gamma}_{3,\mathrm{zero}}$ and $\tilde{\gamma}_{3,\mathrm{pole}}$ increases, forming a resonance dip. The shift of the resonance from the original resonance position γ_{SPP} experimentally observed with decreasing h is due to the increase in v^2.

According to Eq. (31), the direction of displacements of the resonance parameters from the original SPP propagation constant γ_{SPP} is mainly determined by the sign of parameter p_{12} defined by Eq. (8). In the Otto and Kretschmann configurations, the parameters p^O_{12} and p^K_{12} are defined for the dielectric-metal and metal-dielectric interfaces, respectively. For the same set of materials $p^O_{12} = -p^K_{12}$. According to Eq. (8), the real parts of p^O_{12} and p^K_{12} are negative and positive, respectively. Therefore, the resonance shifts to lower values in the Otto configuration and to higher values in the Kretschmann configuration.

B. Coupled-mode theory

In the previous subsection, we showed that the asymmetric line shapes of SPR in the three-layer structures are manifestations of the Fano interference. In this subsection, we clarify

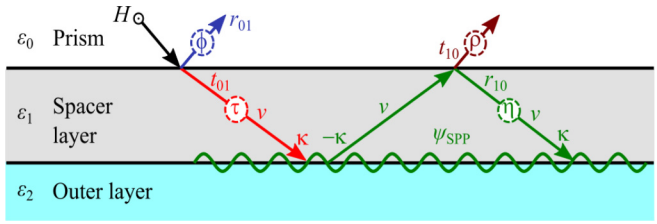

FIG. 4. Transfer processes of coupling and self-coupling between the SPP mode and ingoing and outgoing waves in a three-layer system.

the origins of the interfering flows and provide reasoning for the zero and pole parameters given by Eq. (31). To elucidate the observed interference phenomena, we develop a CM model for the transport processes in three-layer resonance systems. For simplicity, the nonresonant coupling component r_{12}^c at the metal-dielectric interface will be neglected in the following.

As schematically shown by labeled arrows in Fig. 4, the four following transfer processes occur in a three-layer system for an incident plane wave H. The arrow labeled by τ corresponds to the process of incident wave incoupling to the ψ_{SPP} mode. The arrows labeled by η represent a self-interaction of the ψ_{SPP} mode through the back-coupling from the I_{01} interface. Two outcoupling processes, which constitute the total reflected field H_r, include a portion ϕ of the incident wave reflected back into the prism layer without interaction with the structure and a portion ρ of the outcoupled mode field.

Within the CM theory, we can write generalized CM equations to describe the coupling between the ψ_{SPP} mode, ingoing wave H, and outgoing wave H_r:

$$\frac{1}{ik_0\gamma_{SPP}}\frac{d\psi_{SPP}}{dx} = \psi_{SPP} + \eta\psi_{SPP} + \tau H, \tag{33}$$

$$H_r = \phi H + \rho\psi_{SPP}, \tag{34}$$

where γ_{SPP} is the central propagation constant, η is the coefficient expressing the degree of self-interaction or self-coupling of ψ_{SPP} mode, τ expresses the degree of incoupling of the incident wave to the mode, ρ is the coefficient of outcoupling from the mode to the external field, and ϕ describes the portion of the field reflected from the structure without interaction.

The amplitude of ψ_{SPP} is obtained from Eq. (33) under $H \propto \exp(ik_0\alpha x)$ assumption as a Lorentzian:

$$\psi_{SPP} = \frac{\gamma_{SPP}}{\alpha - \gamma_{SPP}(1+\eta)}\tau H. \tag{35}$$

In contrast to the two-layer system, the propagation constant of the mode excited in a three-layer system is perturbed by the mode self-coupling η through the spacer layer that leads to the shift in the propagation constant of the mode determined by the pole parameter $\gamma_{3,pole}^{CM} = \gamma_{SPP}(1+\eta)$. The stronger the self-interaction, the larger the influence on the propagation constant. The mode self-coupling also influences the attenuation of the mode defined by the imaginary part of the perturbed propagation constant.

The reflection coefficient $\tilde{r}_{012} \equiv H_r/H$ is obtained by substitution of Eq. (35) into Eq. (34):

$$\tilde{r}_{012} = \phi\frac{\alpha - \gamma_{SPP}(1+\eta-\rho\tau/\phi)}{\alpha - \gamma_{SPP}(1+\eta)}. \tag{36}$$

The position and depth of the SPR dip are determined by the zero parameter $\gamma_{3,zero}^{CM} = \gamma_{SPP}(1+\eta-\rho\tau/\phi)$. In addition to the influence of self-coupling η of the SPP mode, the resonance dip parameter in a three-layer system is perturbed by the coupling of external fields with the mode and nonresonant reflection from the structure.

The coefficients in Eq. (36) are analytically determined for each transfer process. In the incoupling process, an incident wave H generates an evanescent wave of complex amplitude $t_{01}H$ in the spacer layer at the interface I_{01}. Then, the amplitude of the evanescent wave decays in the spacer layer and becomes $\upsilon t_{01}H$ at the metal-dielectric interface I_{12}. Assuming that the evanescent wave of the amplitude $\upsilon t_{01}H$ incouples to ψ_{SPP} with coupling coefficient κ, the total incoupling degree of H to ψ_{SPP} can be found as $\tau = \kappa\upsilon t_{01}$. In the noninteractive reflection, the portion $r_{01}H$ of the incident wave is reflected back into the prism layer without interaction with the structure that gives $\phi = r_{01}$.

The excited mode ψ_{SPP}, in turn, generates an outcoupled evanescent field of the amplitude $-\kappa\psi_{SPP}$ in the spacer layer at the I_{12} interface. The amplitude of the outcoupled field is attenuated with the decay υ becoming $-\kappa\upsilon\psi_{SPP}$ at the I_{01} interface. At the I_{01} interface, the outcoupled field induces the self-coupling and outcoupling processes. In the self-coupling process, a secondary evanescent wave of the amplitude $-r_{10}\kappa\upsilon\psi_{SPP}$ is generated at I_{01}, attenuated again in the spacer layer with υ, and incoupled to the mode with the coupling coefficient κ. Therefore, the self-interaction coefficient yields $\eta = -\kappa^2\upsilon^2 r_{10}$. In the outcoupling process, the evanescent field outcoupled from the mode of the amplitude $-\kappa\upsilon\psi_{SPP}$ is outcoupled to the propagating wave in the prism with the coefficient t_{10} providing the outcoupling coefficient of $\rho = -\kappa\upsilon t_{10}$.

The reflection coefficient $\tilde{r}_{012}$ for the considered three-layer systems is obtained by substitution of the aforementioned transfer coefficients into Eq. (36) as

$$\tilde{r}_{012} = r_{01}\frac{\alpha - \gamma_{SPP}(1+\upsilon^2\kappa^2/r_{01})}{\alpha - \gamma_{SPP}(1+r_{01}\upsilon^2\kappa^2)}. \tag{37}$$

Taking into account the expression (23) for κ obtained in a two-layer system case, we see that the approximation (37) for the reflection coefficient derived by the CM theory coincides with the approximation (32) obtained by the exact electromagnetic theory, and the expressions for resonance parameters $\gamma_{3,zero}^{CM}$ and $\gamma_{3,pole}^{CM}$ are equal to those in Eq. (31).

As we see from Eq. (37), the direction of displacements of $\gamma_{3,zero}^{CM}$ and $\gamma_{3,pole}^{CM}$ from the original SPP propagation constant γ_{SPP} is determined by the sign of κ^2. Since κ is imaginary for dielectric-metal interfaces and real for metal-dielectric interfaces, the Otto and Kretschmann configurations are characterized by negative and positive values of κ^2, respectively. Therefore, the shift of the resonance parameters to lower and higher values in the Otto and Kretschmann configurations, respectively, is originated from the $\pi/2$ phase difference in their coupling coefficients κ.

C. Comparison of numerical results

In this subsection, we compare reflectivity spectra for the Ag- and Al-based three-layer structures obtained by the

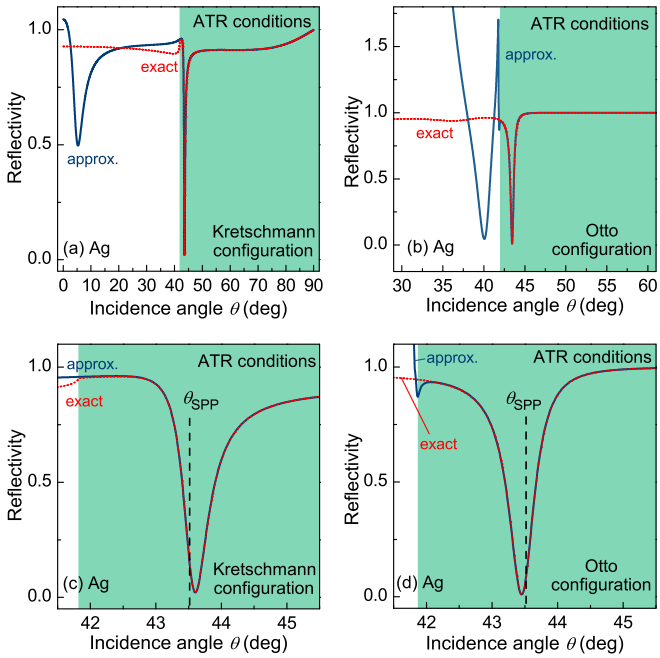

FIG. 5. Fano resonances in exact (dotted line) and approximated (solid line) spectra of reflectivity by three-layer structures in the (a, c) Kretschmann and (b, d) Otto configurations based on Ag. (a, b) The general view and (c, d) the expanded scale near the resonance region. The filled area corresponds to the ATR angular region ($\theta > \theta_c = 41.8^\circ$).

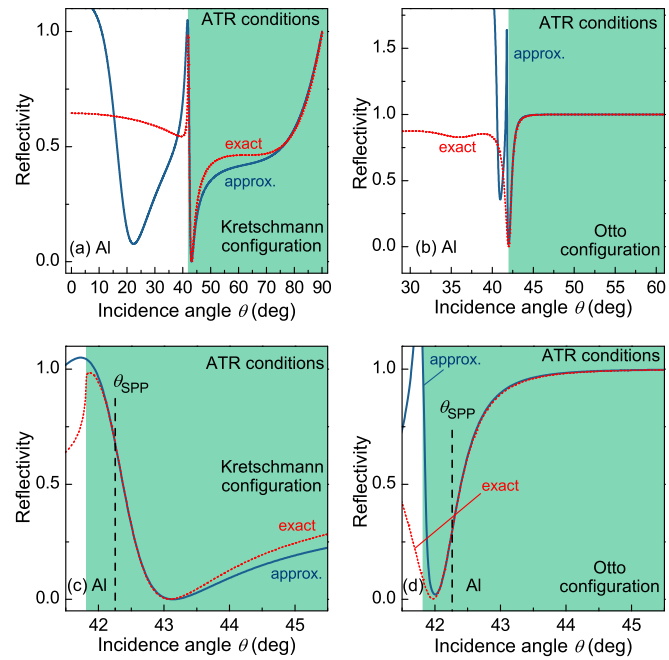

FIG. 6. Fano resonances in exact (dotted line) and approximated (solid line) spectra of reflectivity by three-layer structures in the (a, c) Kretschmann and (b, d) Otto configurations based on Al. (a, b) The general view and (c, d) the expanded scale near the resonance region. The filled area corresponds to the ATR angular region ($\theta > \theta_c$).

approximation (28) with those obtained by the exact expression (24) at $\lambda_0 = 632.8$ nm. In the calculations, we used the constants of materials generally used in the Kretschmann (glass/metal/air) and Otto (glass/air/metal) configurations. The permittivity for the glass layer was taken as $\varepsilon_0 = 2.25$. Thicknesses of the spacer layers h were optimized in order to minimize the reflectivities at resonances. The thicknesses h used in calculations are 50 nm for the glass/Ag/air case, 10 nm for the glass/Al/air case, and 800 nm for both the glass/air/Ag and glass/air/Al cases.

In the Ag case presented in Fig. 5, the results of exact calculations are reproduced very well by the approximate calculations in the ATR region ($\theta_c > \sin^{-1}\sqrt{1/\varepsilon_0}$). It should be noted that the SPR dip in the Kretschmann configuration is located at an angle higher than that in the Otto configuration. In fact, the resonance angle $\theta_{\rm SPP} = \sin^{-1}(\gamma'_{\rm SPP}/\varepsilon_0^{1/2})$ corresponding to the SPP wave number for the two-layer structure of 43.52° is located between the resonance angles $\theta_{\rm min}$ corresponding to the minimum values of the SPR dips for the Kretschmann and Otto configurations.

In the Al case demonstrated in Fig. 6, the fitting is good for the Otto configuration in the whole ATR region, whereas for the Kretschmann configuration the region of good fitting is limited to a narrow region near the resonance (approximately within ±0.5°). The resonance angle corresponding to $\gamma'_{\rm SPP}$ of a SPP mode at a single air/Al interface is found to be $\theta_{\rm SPP} = 42.26^\circ$. Similar to the Ag case, the SPR resonance dips in the Kretschmann and Otto configurations are shifted to the higher and lower values from $\theta_{\rm SPP}$, respectively.

As shown in the above, the shift of the SPR dips in the ATR spectra for the considered configurations in opposite directions is validated by the numerical simulations. According to Eq. (31), the full width at half maximum (FWHM) of SPR dips determined by the imaginary part of a pole parameter is also affected by the SPP mode self-interaction supported by the near field back coupling from the prism interface. Therefore, the shape and position of the minimum of a SPR dip observed in the reflection spectra of the multilayer structures can characterize the propagation constant of a SPP mode, which is supported by metal-dielectric interfaces, only indirectly and approximately.

The resonance parameters obtained from the approximations and exact solutions of reflectivity spectra are summarized in Table II. The pole $\gamma_{3,\rm pole}$ and zero $\gamma_{3,\rm zero}$ parameters are obtained by Eq. (30). The type of configuration affects the values of each parameter for a given metal. As discussed in the previous subsection, Re $\gamma_{3,\rm pole}$ and Re $\gamma_{3,\rm zero}$ are lower and larger than $\gamma'_{\rm SPP}$ for the Otto and Kretschmann configurations, respectively. The incidence angles corresponding to the positions of resonance dips in the approximated $\theta_{\rm zero} = \sin^{-1}({\rm Re}\,\gamma_{3,\rm zero}/\varepsilon_0^{1/2})$ and in exact cases $\theta_{\rm min}$ agree very well in both configurations for both metals, although the difference between them is larger in the Al case. Theoretical values of the approximate line shape width $\Gamma + b''$ are calculated using Eq. (27). They are close to each other for both configurations and agree well with the FWHMs (in RIU) of exact solution. In the Al case, the resonance is close to the critical angle in the Otto configuration that makes the estimation of FWHM difficult.

Note that the resonance peaks are not apparent for the three-layer structures as sharp peaks in ATR spectra of two-layer

TABLE II. Fano resonance parameters for three-layer structures.

Base metal	Configuration	$\gamma_{3,\text{pole}}$ (RIU)	$\gamma_{3,\text{zero}}$ (RIU)	θ_{zero}	θ_{min}	$\Gamma + b''$ (RIU)	FWHM (RIU)
Ag	Kretschmann	$1.033629 + 0.00434i$	$1.034452 - 0.000667i$	43.60°	43.60°	0.0084	0.0086
Ag	Otto	$1.031400 + 0.00407i$	$1.031652 - 0.000406i$	43.45°	43.45°	0.0090	0.0089
Al	Kretschmann	$1.009123 + 0.013382i$	$1.02570 - 0.00064i$	43.14°	43.09°	0.0269	0.0238
Al	Otto	$1.002061 + 0.00222i$	$1.00300 - 0.00036i$	41.96°	41.97°	0.044	

structures. For the considered three-layer structures $\text{Re}\,\gamma_{3,\text{pole}}$ and $\text{Re}\,\gamma_{3,\text{zero}}$ are close to each other that causes a strong interference between the peak and dip resonances. Assuming the same representation of reflectivity as in Eq. (17), we can conclude that if $|\,\text{Im}\,\gamma_{3,\text{pole}}|$ is comparable to or larger than the distance $|\,\text{Re}\,\gamma_{3,\text{pole}} - \text{Re}\,\gamma_{3,\text{zero}}|$ between the positions of the peak and dip, the dip is formed clearly, whereas the peak is not pronounced as can be seen in Fig. 5.

IV. CONCLUSIONS

In the present paper on the resonance response of planar plasmonic structures, we revealed a number of notable phenomena. In particular, near field enhancement spectra at metal-dielectric interfaces demonstrate asymmetrical line shapes. According to the approximations of the spectra, the near field enhancement is composed of resonant and nonresonant components. The narrow resonant component is related to the resonant excitation of SPP modes. The interference of the nonresonant and resonant components results in the asymmetric Fano line shape in near field enhancement spectra. According to the approximations, the position and height of the resonances are determined by the material properties of the layers. Therefore, the appearance of Fano resonances in the near field enhancement spectra of metal-dielectric interfaces is an intrinsic phenomenon.

For the three-layer structures in the Kretschmann and Otto configurations, we demonstrated that the asymmetric resonances in ATR spectra commonly regarded as SPP resonances are actually not a result of trivial excitation of the SPP mode at the metal-dielectric interface. We derived Fano-type analytical expressions for spectral line shapes that revealed existence and origins of interfering nonresonant continuum and resonant components. The remarkable feature of the three-layer structures is the SPP mode self-interaction, which is supported by the spacer layer. Notably, the self-interaction, which can be tuned by the thickness of the spacer layer, results in the shifts of the SPP resonance dip in opposite directions from the intrinsic values for the Kretschmann and Otto configurations.

We numerically demonstrated that near the SPP resonance the approximate Fano expressions reproduce well the spectra calculated by the exact expressions. Implementation of both the electromagnetic and CM theories to the resonance response analysis revealed the role of intrinsic mode losses in the formation of an asymmetric resonance line shape. Another noteworthy conclusion from the CM models is that nonresonant components are not originated from the resonant excitation of SPP modes. The appearance of nonresonant components in the two-layer case is not yet clear and will be the subject of future research. The insight into generation of the resonance response provides a basis for more strict theoretical studies and modeling and characterization of processes in plasmonic materials and devices. The obtained results may be utilized in both the development of numerical methods and the characterization of experimental results in such fields as material science, plasmonics, sensing, and enhanced spectroscopies.

ACKNOWLEDGMENTS

This paper was supported by the Federal Agency of Scientific Organizations (Grant No. 007-GZ/Ch3363/26) (numerical modeling), by the Russian Science Foundation (Grant No. 14-19-00796) (CM model), and by the Russian Foundation for Basic Research (Grant No. 18-07-00613) (EM model).

[1] V. M. Agranovich and D. L. Mills, *Surface Polaritons: Electromagnetic Waves at Surfaces and Interfaces* (North-Holland, Amsterdam, 1982).
[2] A. D. Boardman, *Electromagnetic Surface Modes* (Wiley, New York, 1982).
[3] S. Jahani and Z. Jacob, Nat. Nanotechnol. **11**, 23 (2016).
[4] M. Z. Alam, J. S. Aitchison, and M. Mojahedi, Laser Photon. Rev. **8**, 394 (2014).
[5] S. Hayashi, D. V. Nesterenko, and Z. Sekkat, J. Phys. D: Appl. Phys. **48**, 325303 (2015).
[6] S. Hayashi, Y. Fujiwara, B. Kang, M. Fujii, D. V. Nesterenko, and Z. Sekkat, J. Appl. Phys. **122**, 163103 (2017).
[7] R.-M. Ma, R. F. Oulton, F. J. Sorger, and X. Zhang, Laser Photon. Rev. **7**, 1863 (2013).
[8] R. R. Chance, A. Prock, and R. Silbey, in *Advances in Chemical Physics*, edited by I. Prigogine and Stuart A. Rice (John Wiley and Sons, New York, 1978), Vol. 37, p. 1.
[9] A. Neogi, C.-W. Lee, H. O. Everitt, T. Kuroda, A. Tackeuchi, and E. Yablonovitch, Phys. Rev. B **66**, 153305 (2002).
[10] Y. C. Jun, R. D. Kekatpure, J. S. White, and M. L. Brongersma, Phys. Rev. B **78**, 153111 (2008).
[11] S. A. Maier, *Plasmonics Fundamentals and Applications* (Springer, New York, 2007).
[12] S. Hayashi and T. Okamoto, J. Phys. D **45**, 433001 (2012).
[13] Z. Sekkat, S. Hayashi, D. V. Nesterenko, A. Rahmouni, S. Refki, H. Ishitobi, Y. Inouye, and S. Kawata, Opt. Express **24**, 20080 (2016).
[14] P. Berini, Adv. Opt. Photonics **1**, 484 (2009).

[15] S. Refki, S. Hayashi, A. Rahmouni, D. V. Nesterenko, and Z. Sekkat, Plasmonics **11**, 433 (2015).
[16] S. Hayashi, D. V. Nesterenko, and Z. Sekkat, Appl. Phys. Express **8**, 022201 (2015).
[17] D. V. Nesterenko, S. Hayashi, and Z. Sekkat, J. Opt. **18**, 065004 (2016).
[18] S. Hayashi, D. V. Nesterenko, A. Rahmouni, and Z. Sekkat, Appl. Phys. Lett. **108**, 051101 (2016).
[19] S. Hayashi, D. V. Nesterenko, A. Rahmouni, Z. Sekkat, H. Ishitobi, Y. Inouye, and S. Kawata, Sci. Rep. **6**, 33144 (2016).
[20] S. Hayashi, D. V. Nesterenko, A. Rahmouni, and Z. Sekkat, Phys. Rev. B **95**, 165402 (2017).
[21] P. Berini, New J. Phys. **10**, 105010 (2008).
[22] C. Nylander, B. Liedberg, and T. Lind, Sens. Actuators **3**, 79 (1982).
[23] J. Homola, Chem. Rev. **108**, 462 (2008).
[24] D. V. Nesterenko and Z. Sekkat, Plasmonics **8**, 1585 (2013).
[25] M. Zekriti, D. V. Nesterenko, and Z. Sekkat, Appl. Opt. **54**, 2151 (2015).
[26] S. A. Meyer, E. C. Le Ru, and P. G. Etchegoin, Anal. Chem. **83**, 2337 (2011).
[27] S. Hayashi, A. Maekawa, S. C. Kim, and M. Fujii, Phys. Rev. B **82**, 035441 (2010).
[28] M. I. Stockman, Opt. Express **19**, 22029 (2011).
[29] T. Zhu, Y. Zhou, Y. Lou, H. Ye, M. Qiu, Z. Ruan, and S. Fan, Nat. Commun. **8**, 15391 (2017).
[30] M. Puiu and C. Bala, Sensors **16**, 870 (2016).
[31] H. Kim, J. Hahn, and B. Lee, Opt. Express **16**, 3049 (2008).
[32] E. A. Bezus, L. L. Doskolovich, N. L. Kazanskiy, V. A. Soifer, and S. I. Kharitonov, J. Opt. **12**, 015001 (2010).
[33] E. A. Bezus, L. L. Doskolovich, and N. L. Kazanskiy, Opt. Express **22**, 13547 (2014).
[34] Z. Ruan, H. Wu, M. Qiu, and S. Fan, Opt. Lett. **39**, 3587 (2014).
[35] H. Raether, *Surface Plasmons on Smooth and Rough Surfaces and on Gratings* (Springer-Verlag, Berlin, 1988).
[36] S. Kawata, Jpn. J. Appl. Phys. **52**, 010001 (2013).
[37] D. Barchiesi and A. Otto, La Rivista del Nuovo Cimento **36**, 173 (2013).
[38] T. Turbadar, Proc. Phys. Soc. **73**, 40 (1959).
[39] T. Turbadar, Opt. Acta **11**, 207 (1964).
[40] A. Otto, Z. Phys. A **216**, 398 (1968).
[41] E. Kretschmann and H. Raether, Z. Naturforsch. A **23**, 2135 (1968).
[42] E. Kretschmann, Z. Phys. A **241**, 313 (1971).
[43] K. Kurihara, K. Nakamura, and K. Suzuki, Sens. Actuators B **86**, 49 (2002).
[44] A. Miroshnichenko, Y. S. Kivshar, and S. Flach, Rev. Mod. Phys. **82**, 2257 (2010).
[45] U. Fano, Nuovo Cimento **12**, 154 (1935).
[46] U. Fano, Phys. Rev. **124**, 1866 (1961).
[47] B. Gallinet and O. J. F. Martin, ACS Nano **5**, 8999 (2011).
[48] B. Gallinet and O. J. F. Martin, Phys. Rev. B **83**, 235427 (2011).
[49] S. Collin, Rep. Prog. Phys. **77**, 126402 (2014).
[50] W. Zhou, D. Zhao, Y.-C. Shuai, H. Yang, S. Chuwongin, A. Chadha, J.-H. Seo, K. X. Wang, V. Liu, Z. Ma, and S. Fan, Prog. Quantum Electron. **38**, 1 (2014).
[51] Y. S. Joe, A. M. Satanin, and C. S. Kim, Phys. Scr. **74**, 259 (2006).
[52] H. A. Haus, *Waves and Fields in Optoelectronics* (Prentice-Hall, Englewood Cliffs, NJ, 1984).
[53] S. Fan, W. Suh, and J. D. Joannopoulos, J. Opt. Soc. Am. A **20**, 569 (2003).
[54] D. A. Bykov, L. L. Doskolovich, and V. A. Soifer, Opt. Express **25**, 1151 (2017).
[55] Z. Ruan and S. Fan, J. Phys. Chem. C **114**, 7324 (2010).
[56] Z. Ruan, Opt. Lett. **40**, 601 (2015).
[57] P. Yeh, A. Yariv, and C.-S. Hong, J. Opt. Soc. Am. **67**, 423 (1977).
[58] Y. Lou, H. Pan, T. Zhu, and Z. Ruan, J. Opt. Soc. Am. B **33**, 819 (2016).
[59] E. D. Palik, *Handbook of Optical Constants of Solids* (Academic, Orlando, 1985).
[60] A. D. Rakic, A. B. Djurisic, J. M. Elazar, and M. L. Majewski, Appl. Opt. **37**, 5271 (1998).